Available online at www.sciencedirect.com
ScienceDirect
Intermetallics 16 (2008) 373–377
Intermetallics
www.elsevier.com/locate/intermet

Phase relations and stabilities at 900 °C in the U–Fe–Si ternary system

D. Berthebaud [a], O. Tougait [a,*], A.P. Gonçalves [b], H. Noël [a]

[a] *Sciences Chimiques de Rennes, Equipe Chimie du Solide et Matériaux, UMR CNRS 6226, Université de Rennes 1, 263 Avenue de Général Leclerc, 35042 Rennes, France*
[b] *Departamento de Química, Instituto Tecnológico e Nuclear/CFMC-UL, P-2686-953 Sacavém, Portugal*

Received 9 November 2007; received in revised form 16 November 2007; accepted 23 November 2007
Available online 11 January 2008

Abstract

A systematic study of the U–Fe–Si ternary system was carried out in the whole concentration range, by means of scanning electron microscope observations, associated with energy dispersive X-ray spectroscopy analyses and X-ray powder diffraction measurements performed on as-cast and annealed samples. At 900 °C, the phase diagram is characterized by the existence of nine ternary compounds: U_2FeSi_3 with the AlB_2-type, UFe_2Si_2 with the $ThCr_2Si_2$-type, $U_3Fe_2Si_7$ with the $La_3Co_2Sn_7$-type, U_2Fe_3Si with the $MgZn_2$-type, UFeSi with the TiNiSi-type, $U_{1.2}Fe_4Si_{9.7}$ with the $Er_{1.2}Fe_4Si_{9.7}$-type, $U_2Fe_3Si_5$ with the $Lu_2Co_3Si_5$-type, $U_6Fe_{16}Si_7$ of the $Mg_6Cu_{16}Si_7$-type and UFe_5Si_3 with its own type of structure. Two intermediate solid solutions, $U_2Fe_{17-x}Si_x$ ($3.2 < x < 4$) structurally related to the Th_2Ni_{17}-type and $UFe_{12-x}Si_x$ ($1 < x < 3$) structurally related to the $ThMn_{12}$-type are formed and two extensions of binaries into the ternary system, UFe_xSi_{2-z-x} ($0 < x < 0.2$) and UFe_xSi_{1-x} ($0 < x < 0.05$) are observed. The homogenous ranges are formed by Si/Fe mechanisms of substitution. Analyses on as-cast samples revealed the formation of two additional ternary phases which were found to be stable only at high temperature, $UFe_{1-x}Si_2$ with $x = 0.8$ and a novel ternary compound with a 18(1)U:59(1)Fe:23(1)Si estimated atomic ratio.

Keywords: A. Ternary alloy systems; B. Crystal chemistry of intermetallics; B. Phase diagrams; B. Phase identification; F. Electron microprobe

1. Introduction

Uranium based intermetallics are known to display competing interactions which may yield at low temperature to the formation of heavy fermion ground states [1]. The thermoelectrical power of these systems exhibits complex temperature dependence [2] which is characterized by positive or negative peaks at temperatures of the order of the overall crystal field splitting or of the Kondo temperature [3]. The absolute values of the Seebeck coefficient (S) at the vicinity of these anomalies usually exceed those characteristics of simple metals by about 10–100 times. Numerous studies suggest that these enhanced thermopower values are mostly controlled by interatomic distances and chemical substitutions [4] which directly influence the hybridisation between the uranium 5f states and the s-, p- or d-states of the neighbouring atoms. In this respect, the intermetallic systems combining U and Fe have to be considered of great interest due to the substantial degree of delocalisation of the U 5f-electrons that directly hybridise with the Fe 3d-electrons [5].

The main interest of the present research project is the thorough examination of the U–Fe–Si ternary system by a careful evaluation of the electronic properties of the intermediate phases, in relation with the chemical composition. The temperature dependences of the electrical resistivity and thermopower of $U_3Fe_2Si_7$, U_2FeSi_3, $U_{1.2}Fe_4Si_{9.7}$, $U_2Fe_3Si_5$ and UFe_2Si_2 ternary phases have been recently presented [6]. The novel intermediate phases UFe_5Si_3 [7] and $U_6Fe_{16}Si_7$ [8] have been structurally characterized, and their magnetic and transport properties measured. As a final step on the crystal-chemistry investigation of the intermediate phases of the U–Fe–Si ternary system, we present here the assessment in an extended concentration range of the isothermal section of

* Corresponding author. Tel.: +33 2 23 23 57 40; fax: +33 2 23 23 67 99.
E-mail address: tougait@univ-rennes1.fr (O. Tougait).

0966-9795/$ - see front matter © 2007 Elsevier Ltd. All rights reserved.
doi:10.1016/j.intermet.2007.11.007

this phase diagram at 900 °C as well as information about the phase formation.

2. Literature data

2.1. Binary systems

A total of 14 intermediate binary phases and 2 solid solutions based on the elements are reported to exist in the binary boundary systems at 900 °C. Crystallographic and some thermodynamic data about the binary phases of the uranium–silicon, uranium–iron and iron–silicon systems are gathered in Table 1. The data about the binary uranium silicides are issued from previous reinvestigations [9,10] revising the currently accepted compilation [11]. This binary system comprises six well-defined compounds, U_3Si, U_3Si_2, U_5Si_4, USi, USi_2 and USi_3, and non-stoichiometric phases, between the compositions U_3Si_5 ($USi_{1.67}$) and USi_{2-z} ($USi_{1.88}$). The stoichiometric compound USi_2 has a peritectoid decomposition above 450 °C and was not further considered in the present study. Methodic examinations have revealed the occurrence of the non-stoichiometric phases; U_3Si_5 crystallizing with the hexagonal defect AlB_2-type as well as a phase separation into two orthorhombically distorted AlB_2-type related phases (o1-U_3Si_{5+y} and o2-U_3Si_{5+y}), USi_{2-z} with the orthorhombic defect $GdSi_2$-type at its silicon poor phase boundary and USi_{2-z} with the tetragonal defect $ThSi_2$ type structure at its silicon rich phase boundary. In agreement with previous assessment of ternary phase diagram involving the U–Si binary system [12,13], we consider individual phases between U_3Si_5 and USi_{2-z}. The U–Fe phase diagram is well known and has been taken from Ref. [14], in this system two compounds form, UFe_2 ($MgCu_2$-type) and U_6Fe (U_6Mn-type), without significant solubility ranges. U_6Fe has a melting temperature about 805 °C. At $T = 900$ °C, the Fe–Si system [11] shows three well-defined compounds, Fe_5Si_3, FeSi and β-$FeSi_2$. Two additional solid solutions α1 and α2 are reported, they correspond at this temperature to the dissolution of Si in Fe in the range 17–27.3% and 13.4–17%, respectively.

2.2. Ternary phases

The following ternary intermetallic compounds were previously reported from the literature: U_2FeSi_3 (AlB_2-type) [15], UFe_2Si_2 (Al_4Ba-type) [16], $U_3Fe_2Si_7$ ($La_3Co_2Sn_7$-type) [17], U_2Fe_3Si ($MgZn_2$-type) [18], $UFe_{12-x}Si_x$ ($ThMn_{12}$-type) [19], UFeSi (TiNiSi-type) [20], $U_{1.2}Fe_4Si_{9.7}$ ($Er_{1.2}Fe_4Si_{9.7}$-type) [21], $U_2Fe_3Si_5$ ($Lu_2Co_3Si_5$-type) [22], $U_2Fe_{17-x}Si_x$ (Th_2Ni_{17}-type) [23] and $UFe_{0.8}Si_2$ ($CeNiSi_2$-type) [24]. Their crystallographic data are presented in Table 2 and, as the formation of all of them were confirmed in this work, they are discussed below, in Section 4.

3. Experimental

Starting materials were uranium turnings (nuclear grade), iron pieces (Strem, 5N) and silicon (Strem, 6N). Samples with xU:yFe:zSi nominal compositions were prepared by melting the calculated amounts of the elements in an arc furnace, under a high purity argon atmosphere. The surface of the

Table 1
Data for the binary phases taken from the U–Si, U–Fe and Fe–Si systems

Phase	Transformation temperature[a] (°C)	Space group	Structure type	Lattice parameters (Å)			Ref.
				a	*b*	*c*	
U_3Si (γ)	930, mp	*Pm*-3*m*	Cu_3Au	4.346	–	–	[11]
U_3Si (β)	762, t	*I*4/*mcm*	U_3Si (β)	6.0328	–	8.6907	[11]
U_3Si (α)	−153, t	*Fmmm*	U_3Si (α)	8.654	8.549	8.523	[11]
U_3Si_2	1665, mp	*P*4/*mbm*	U_3Si_2	7.3299	–	3.9004	[11]
U_5Si_4		*P*6/*mmm*	$U_{20}Si_{16}C_3$	10.467	–	7.835	[10]
USi	1580, mp	*I*4/*mmm*	USi	10.58	–	24.31	[9]
USi[b]		*Pnma*	FeB	7.585	3.903	5.663	[9]
U_3Si_5	1770, mp	*P*6/*mmm*	AlB_2	3.843	–	4.069	[11]
o1-U_3Si_5 (at 63 at.% Si)		*Pmmm*	Dist. AlB_2	3.869	6.660	4.073	[9]
o2-U_3Si_5 (at ∼63 at.% Si)		*Pmmm*	Dist. AlB_2	3.893	6.717	4.042	[9]
USi_{2-z} (at 64 at.% Si)		*Imma*	Defect $GdSi_2$	3.953	3.929	13.656	[9]
USi_{2-z} (at 65 at.% Si)	1710, mp	$I4_1/amd$	Defect $ThSi_2$	3.9423	–	13.712	[9,11]
USi_2	450	$I4_1/amd$	$ThSi_2$	3.922	–	14.154	[11]
USi_3	1510, mp	*Pm*-3*m*	Cu_3Au	4.060	–	–	[11]
UFe_2	1235, mp	*Fd*-3*m*	$MgCu_2$	7.055(2)	–	–	[14]
U_6Fe	805, p	*I*4/*mcm*	U_6Mn	10.3022(1)	–	5.2386(1)	[14]
Fe_3Si (α1)		*Fm*-3*m*	BiF_3	5.650	–	–	[11]
Fe_3Si (α2)		*Pm*-3*m*	CsCl	2.81	–	–	[11]
Fe_2Si	1212, mp	*P*-3*m*1	Fe_2Si	4.052(2)	–	5.0855(3)	[11]
Fe_5Si_3	1060, pt	$P6_3/mcm$	Mn_5Si_3	6.7416	–	4.7079	[11]
FeSi	1410, mp	$P2_13$	FeSi	4.483	–	–	[11]
$FeSi_2$ (α)	1220, mp	*Cmca*	α$FeSi_2$	2.6901	–	5.134	[11]
$FeSi_2$ (β)	982, pt	*P*4/*mmm*	β$FeSi_2$	9.863	7.791	7.833	[11]

[a] t = solid state transition, mp = melting point, p = peritectic reaction, pt = peritectoid reaction.
[b] Probably oxygen stabilized.

Table 2
Crystallographic data for the ternary U–Fe–Si compounds and solid solutions stable at 900 °C

Compound: composition (solid solution)	Structure type	Space group	Lattice parameters (Å)			Ref.
			a	*b*	*c*	
A: U_2FeSi_3	AlB_2	*P6/mmm*	4.01	–	3.84	[15]
			4.011(4)		3.864(5)	This work
B: UFe_2Si_2	$ThCr_2Si_2$	*I4/mmm*	3.951	–	9.53	[16]
			3.946(2)		9.540(3)	This work
C: $U_3Fe_2Si_7$	$La_3Co_2Sn_7$	*Cmmm*	4.020(1)	24.367(8)	4.028(1)	[17]
			4.013(4)	24.324(1)	4.023(1)	This work
D: U_2Fe_3Si	$MgZn_2$	*P6$_3$/mmc*	5.145	–	7.717	[18]
			5.154(1)	–	7.686(1)	This work
E: $UFe_{12-x}Si_x$ ($x = 1$–3)	$ThMn_{12}$	*I4/mmm*	8.379 (for $x = 1$)	–	4.726	[19]
			8.350(6) (for $x = 2$)	–	4.705(1)	This work
F: $U_2Fe_{17-x}Si_x$ ($x = 3.3$–4.5)	Th_2Ni_{17}	*P6$_3$/mmc*	8.349 (for $x = 3.3$)	–	8.18	[23]
$U_2Fe_{17-x}Si_x$ ($x = 3.2$–4)	Th_2Ni_{17}	*P6$_3$/mmc*	8.330(1) (for $x = 3.2$)	–	8.201(1)	This work
G: UFeSi	TiNiSi	*Pnma*	6.997(2)	4.063(1)	6.867(2)	[20]
			7.001(5)	4.065(1)	6.857(1)	This work
H: $U_{1.2}Fe_4Si_{9.7}$	$Er_{1.2}Fe_4Si_{9.7}$	*P6$_3$/mmc*	3.956(1)	–	15.055(2)	[21]
			3.960(1)	–	15.075(5)	This work
I: $U_2Fe_3Si_5$	$Lu_2Co_3Si_5$	*C2/c*	10.848 $\beta = 119.4$	11.476	5.518	[22]
			10.843(5) $\beta = 119.38$	11.482(5)	5.163(5)	This work
J: UFe_5Si_3	UFe_5Si_3	*P4/mmm*	3.9296(5)	–	7.7235(1)	[7]
K: $U_6Fe_{16}Si_7$	$Mg_6Cu_{16}Si_7$	*Fm-3m*	11.7206(5)	–	–	[8]
			11.7817(5)	–	–	This work
UFe_xSi_{1-x} ($x = 0$–0.05)	USi	*I4/mmm*	10.5889 (for $x = 0.05$)	–	24.3020	This work
UFe_xSi_{2-z-x} ($x = 0$–0.2)	Def. $ThSi_2$	*I4$_1$/amd*	3.9409 (for $x = 0.2$)	–	13.6694	This work

uranium turnings was cleaned in diluted nitric acid prior to melting. To ensure good homogeneity, the samples were re-melted three times. The ingots with aweight loss higher than 1% were not further investigated. Heat-treatments were carried out in evacuated fused silica tubes which were sealed under residual atmosphere of argon. The reaction tubes were annealed at 900 °C for 15 days. Powder X-ray diffraction (XRD) patterns of the samples were collected at room temperature using Co Kα radiation on an Inel CPS 120 diffractometer, equipped with a position-sensitive detector covering 120° in 2θ with a resolution of 0.03°. The POWDERCELL software package [25] was used to compare the experimental diffractograms with the ones generated for the known compounds and to calculate the refined unit-cell parameters.

The microstructures were observed on polished surfaces using a Jeol JSM 6400 scanning electron microscope (SEM), equipped for energy dispersive X-ray spectroscopy (EDS). At least three EDS point analysis were obtained for each phase. Automated matrix corrections were performed by standard EDS software. To obtain a more precise evaluation of the chemical composition of the phases, binary or ternary compounds without solubility range and that were previously unambiguously identified by X-ray diffraction were used as standards.

4. Results

The isothermal section at 900 °C of the U–Fe–Si ternary phase diagram is shown in Fig. 1. It has been constructed by using the experimental results obtained from the X-ray powder diffraction experiments, observations by scanning electron microscopy coupled with EDS analyses. The relevant crystallographic data along with the homogeneity ranges of the ternary U–Fe–Si intermediate phases are gathered in Table 2. The liquid phase (L) in the ternary system was evaluated according to the liquid phase expansions within the binary system U–Fe [11] and the junction between several points of analysis.

The existence and composition of 10 binary phases previously reported to be stable at 900 °C were confirmed and their

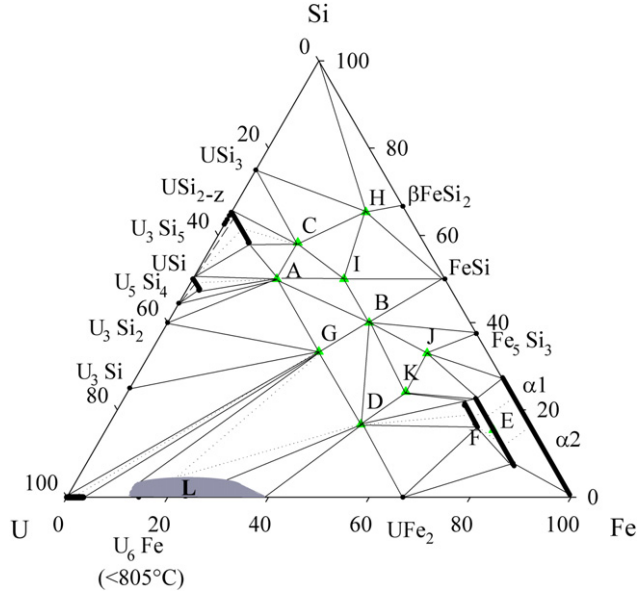

Fig. 1. Isothermal section at 900 °C of the U–Fe–Si system: (A) U_2FeSi_3, (B) UFe_2Si_2, (C) $U_3Fe_2Si_7$, (D) U_2Fe_3Si, (E) $UFe_{12-x}Si_x$ ($1 < x < 3$), (F) $U_2Fe_{17-x}Si_x$ ($3.2 < x < 4$), (G) UFeSi, (H) $U_{1.2}Fe_4Si_{9.7}$, (I) $U_2Fe_3Si_5$, (J) UFe_5Si_3 and (K) $U_6Fe_{16}Si_7$. Dash tie-lines are extrapolations.

crystallographic analysis agrees with the literature data. Regarding the limits of the homogeneity ranges of the solid solutions, α1 and α2, of the Fe–Si binary system, our analyses roughly confirm the reported values. At 900 °C, the solubility of Fe in γ-U, estimated at 4 at.% Fe, compares well with the reported value [11]. It is worthwhile mentioning that (U,Fe) solid solution easily retains at room temperature the metastable γ-form, by quenching from 900 °C. Two binary extensions into the ternary system were observed and their limit of solubility evaluated; UFe_xSi_{1-x} $(0 < x < 0.05)$ based on the USi compound and UFe_xSi_{2-z-x} $(0 < x < 0.2)$ with the defect $ThSi_{2-x}$ type of structure. The homogenous ranges based on binary compounds are governed by a mechanism of substitution of Si by Fe, only. All the other binary phases were found to have negligible extension into the ternary system. The area defined by U_3Si_2–USi_3–$U_3Fe_2Si_7$–U_2FeSi_3 is characterized by the occurrence of five three-phase fields, four two-phase fields and two single-phase fields. The determination of the phase equilibria in the USi–USi_{2-z}–$USi_{2-z-y}Fe_y$ was severely hindered by the narrowness of the phase fields of about 1 or 2 at.% which is of the same order of the accuracy limits of our analyses. For this reason the phase equilibria could not be determined for samples with less than 2 at.% Fe, and the occurrence of the binary phases, U_3Si_5 (AlB_2-type), the two orthorhombically distorted AlB_2-type related phases (o1-U_3Si_{5+y} and o2-U_3Si_{5+y}) and USi_{2-z} (defect $GdSi_2$-type) have not been observed in ternary samples.

Among the reported ternary compounds, seven were found to be stable at 900 °C, (A): U_2FeSi_3, (B): UFe_2Si_2, (C): $U_3Fe_2Si_7$, (D): U_2Fe_3Si, (G): UFeSi, (H): $U_{1.2}Fe_4Si_{9.7}$, and (I): $U_2Fe_3Si_5$. The evaluation of the X-ray powder patterns from heat-treated samples confirmed the previous assignment of the crystal structures. The refinements of the unit-cell dimensions compare well with the data of the literature. Quantitative EDS analyses revealed that they do not show detectable ranges of solid solubility, indicating that they are point-compounds. The isothermal section is also characterized by the occurrence of two intermediate solid solutions (F): $U_2Fe_{17-x}Si_x$ $(3.2 < x < 4)$ which adopts the Th_2Ni_{17}-type and (E): $UFe_{12-x}Si_x$$(1 < x < 3)$, with the $ThMn_{12}$-type. The homogeneous region $U_2Fe_{17-x}Si_x$ $(3.2 < x < 4)$ evaluated at 900 °C is slightly narrower than that previously announced, $U_2Fe_{17-x}Si_x$ $(3.3 < x < 4.5)$ which was estimated after annealing at 850 °C [23], but supports the assumption of a decomposition of this ternary intermediate phase at higher temperature. In this context, it is interesting to note that uranium and iron do not form binary compounds with the hexagonal Th_2Ni_{17}-type or with the tetragonal $ThMn_{12}$-type, but these structures can be stabilized by chemical alloying using a third element such as silicon.

The systematic investigation of the isothermal section of the U–Fe–Si system allowed us to characterize two new ternary intermediate phases stable at 900 °C, (K): $U_6Fe_{16}Si_7$ and (J): UFe_5Si_3. UFe_5Si_3 crystallizes in the tetragonal space group *P4/mmm* (No. 123) with the lattice parameters $a = 3.9296(5)$ Å and $c = 7.7235(1)$ Å. Its crystal structure appears as a novel atomic arrangement among intermetallic compounds. The structure of UFe_5Si_3 can be viewed as built up from an infinite three-dimensional framework of Fe and Si atoms, which defines tunnels with hexagonal section where the U atoms reside. No evidence for any deviation from stoichiometry could be detected from microprobe analyses and X-ray powder experiments [7]. $U_6Fe_{16}Si_7$ crystallizes in the cubic $Mg_6Cu_{16}Si_7$-type with lattice parameter refined from powder data, $a = 11.7217(5)$ Å, which compares well with the value obtained from single crystal refinement [8]. Its crystal structure defines octahedral voids composed of six uranium atoms, which can easily accommodate interstitial elements such as O or C. On the opposite, insertion of Si or Fe at this position was found not pertinent by EDS and structural analyses.

The known ternary compound $UFe_{0.8}Si_2$ reported to adopt the orthorhombic $CeNiSi_2$-type [24] and was found to be not stable after long-term annealing at 900 °C, whereas its formation was clearly evidenced on as-cast samples. Our XRD and EDS analyses on as-cast samples of $UFe_{0.8}Si_2$ confirm the chemical composition and unit-cell parameters previously published [24]. In this earlier study, the samples were heat-treated at 1000 °C, suggesting therefore, that the $UFe_{0.8}Si_2$ ternary phase starts to decompose in the temperature range 900–1000 °C. Microprobe analyses on as-cast samples containing more than 55 at.% iron, have revealed the formation of a new intermediate phase with U:Fe:Si of 18(1):59(1):23(1) as estimated atomic ratio. The as-cast alloy, with the above given atomic ratio as initial composition, mainly consists of the new phase and dark $U_2Fe_{17-x}Si_x$ grains in the matrix (Fig. 2). After subtraction of the contribution from the hexagonal structure of $U_2Fe_{17-x}Si_x$ (Th_2Ni_{17}-type), the X-ray diffraction pattern shows unindexed reflections which cannot be ascribed to any type of structures commonly encountered. Employing automatic powder indexing programs did not afford relevant unit-cell parameters. After long-term annealing at 900 °C, the examination of the alloys by SEM–EDS analyses and X-ray powder diffraction experiments, reveals a three-phases equilibrium: $U_2Fe_3Si + U_6Fe_{16}Si_7 + U_2Fe_{17-x}Si_x$, indicating that the

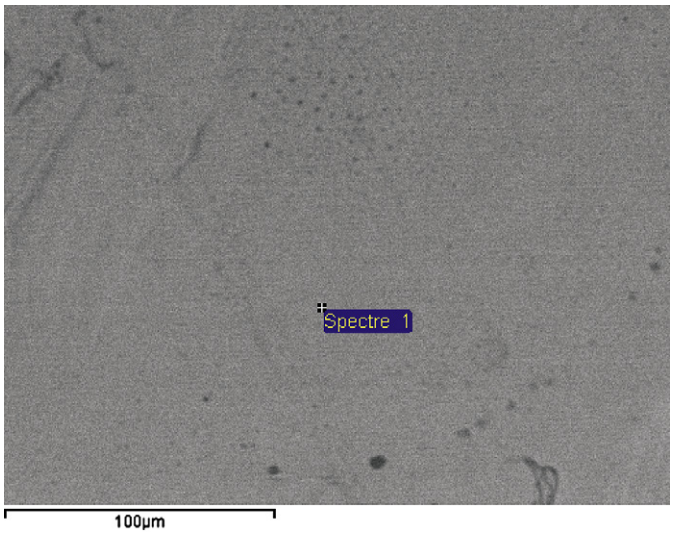

Fig. 2. Back scattered electrons image of the as-cast $U_{18}Fe_{59}Si_{23}$ microstucture.

new phase with the proximate atomic composition $U_{18}Fe_{59}Si_{23}$ is not stable at 900 °C. Further efforts to structurally and chemically characterize this new phase were therefore not attempted.

Comparison of the isothermal sections at 900 °C of the U–Fe–Si ternary system with the Ce–Fe–Si one, recently published [26], affords interesting features about crystal-chemistry of the intermediate phases. For both cases, the homogeneous regions are formed by Fe/Si mechanism of substitutions. The Ce–Fe binaries are able to dissolve silicon, $CeFe_2$ up to 5 at.% Si and Ce_2Fe_{17} up to 16 at.% Si, whereas UFe_2, the only U–Fe binary compound stable at 900 °C, does not. However, in both cases, small substitution of Fe by Si yields solid solutions structurally related to binary types, which are not present in the Ce–Fe and U–Fe systems. For the U-based ternary system, chemical alloying with Si gives two intermediate solid solutions, one structurally related to the $ThMn_{12}$-type, and the second one associated with the Th_2Ni_{17}-type. Two solid solutions deriving from the $NaZn_{13}$-type form in the Ce-based ternary system. It is interesting to note that the binary extension into the Ce–Fe–Si ternary system, $Ce_2Fe_{17-x}Si_x$ ($0 < x < 3$), adopts the Th_2Zn_{17}-type of structure in the whole solubility range. Both the Ce–Fe–Si and U–Fe–Si phase diagrams comprise an intermediate phases with the AlB_2-type and $CeNiSi_2$-type, but with different compositions and thermal behaviours. The U-based compounds are stabilized for stoichiometries with less iron than the Ce-analogues. The formulae are U_2FeSi_3 and $UFe_{0.8}Si_2$ whereas the Ce-based compounds have the formulae $Ce_5Fe_2Si_8$ and $CeFeSi_2$. In addition, $UFe_{0.8}Si_2$ is a high temperature phase, which starts to decompose in the temperature range 900–1000 °C. Both phase diagrams comprise an equiatomic phase, but with a different structure type. UFeSi crystallizes with the orthorhombic TiNiSi-type, whereas CeFeSi adopts a ternary ordered variant of the Cu_2Sb-type.

Finally, it appears that the only shared intermediate phase possess the remarkable composition RFe_2Si_2, where R stands for an f-element. It adopts the $ThCr_2Si_2$-type of structure. A similar conclusion was reached in a previous review [27] on isothermal sections of the ternary systems combining iron, silicon and rare earth element (Y, La, Sm, Gd, Dy [28], Tm [29]).

Acknowledgement

This work was partially supported by the exchange Program GRICES/CNRS 2007–2008.

References

[1] Stewart RG. Rev Mod Phys 1984;56:755.
[2] Behnia K, Jaccard D, Flouquet J. J Phys Condens Matter 2004;16:5187.
[3] Bhattacharjee AK, Coqblin B. Phys Rev B 1976;13:3441.
[4] Wilhelm H, Zlatic V, Jaccard D. Physica B 2006;378–380:644.
[5] Brooks MSS, Eriksson O, Johansson B, Franse JJM, Frings PH. J Phys F 1998;18:L33.
[6] Berthebaud D, Lopes EB, Tougait O, Gonçalves AP, Potel M, Noël H. J Alloys Compd 2007;442:348.
[7] Berthebaud D, Gonçalves AP, Tougait O, Potel M, Lopes EB, Noël H. Chem Mater 2007;19:3441.
[8] Berthebaud D, Tougait O, Potel M, Gonçalves AP, Lopes EB, Noël H. J Solid State Chem 2007;180:2926.
[9] Remschnig K, LeBihan T, Noël H, Rogl P. J Solid State Chem 1992;97:391.
[10] Noël H, Queneau V, Durand JP, Colomb P. In: Abstract of a paper at the international conference on strongly correlated electron systems – SCSES98, 15–18 juillet, Paris; 1998. p. 92.
[11] Massalski TB, Okamoto H, Subramanian PR, Kacprzak L, editors. Binary alloy phase diagrams. 2nd ed., vol. 1–3. ASM International; 1990.
[12] Rogl P, Le Bihan T, Noël H. J Nucl Mater 2001;288:66.
[13] Weitzer F, Rogl P, Noël H. J Alloys Compd 2005;387:246.
[14] Kubaschewski O. Iron-binary phase diagrams. Springer-Verlag; 1982. p. 160.
[15] Pinto M de L. Acta Crystallogr 1966;21:999.
[16] Ban Z, Sikirica M. Z Anorg Allg Chem 1967;356:96.
[17] Aksel'rud LG, YaYarmolyuk P, Rozhdestvenskaya IV, Gladyshevskii EI. Kristallografiya 1981;26:186.
[18] Kusma JB, Nowotny H. Monat Fuer Chemie 1964;95:428.
[19] Andreev AV, Andreev SV, Tarasov EN. J Less-Common Met 1991;167:255.
[20] Canepa F, Manfrinetti P, Pani M, Palenzona A. J Alloys Compd 1996;234:225.
[21] Noguchi S, Okuda K, Abliz M, Goto K, Kindo K, Haga Y, et al. Physica B 1998;246–247:456.
[22] Hickey E, Chevalier B, Gravereau P, Etourneau J. J Magn Magn Mater 1990;90-91:501.
[23] Berlureau T, Gravereau P, Chevalier B, Etourneau J. J Solid State Chem 1993;104:328.
[24] Kaczorowski D. Solid State Commun 1996;99:949.
[25] Kraus W, Nolze G. Powdercell 2.4. Bundesanstalt fuer Materialforschung und -pruefung; 2000.
[26] Berthebaud D, Tougait O, Potel M, Noël H. J Alloys Compd 2007;442:104.
[27] Rogl P. In: Gschneidner Jr KA, Eyring L, editors. Handbook on the physics and chemistry of rare earths. Elsevier Science Publishers B.V.; 1984 [chapter 51].
[28] Yinghong Z, Yiqiang Y, Huaiying Z, Wen Q. J Alloys Compd 1998;268:137.
[29] Müller M, Schmidt H, Braun HF. J Alloys Compd 1997;257:205.